Tetrahydrides of third-row transition elements: Spin-orbit coupling effects on the stability of rhenium tetrahydride

Shiro Koseki,[1,2,a)] Taka-aki Hisashima,[1] Toshio Asada,[1,2] Azumao Toyota,[3] and Nikita Matsunaga[4]
[1]*Department of Chemistry, Graduate School of Science, Osaka Prefecture University, 1-1 Gakuen-cho, Naka-ku, Sakai, Osaka 599-8531, Japan*
[2]*The Research Institute for Molecular Electronic Devices (RIMED), Osaka Prefecture University, 1-1 Gakuen-cho, Naka-ku, Sakai 599-8531, Japan*
[3]*Department of Chemistry, Faculty of Education, Yamagata University, Yamagata 990-8560, Japan*
[4]*Department of Chemistry and Biochemistry, Long Island University, Brooklyn, New York 11201, USA*

(Received 23 July 2010; accepted 10 September 2010; published online xx xx xxxx)

The potential energy surface of low-lying states in rhenium tetrahydride (ReH_4) was explored by using the multiconfiguration self-consistent field (MCSCF) method together with the SBKJC effective core potentials and the associated basis sets augmented by a set of *f* functions on rhenium atom and by a set of *p* functions on hydrogen atoms, followed by spin-orbit coupling (SOC) calculations to incorporate nonscalar relativistic effects. The most stable structure of ReH_4 was found to have a D_{2d} symmetry and its ground state is $^4A_2$. It is found that this is lower in energy than the dissociation limit, ReH_2+H_2, after dynamic correlation effects are taken into account by using second-order multireference Møller–Plesset perturbation (MRMP2) calculations. This reasonably agrees with previous results reported by Andrews *et al.* [J. Phys. Chem. **107**, 4081 (2003)]. The present investigation further revealed that the dissociation reaction of ReH_4 cannot occur without electronic transition from the lowest quartet state to the lowest sextet state. This spin-forbidden transition can easily occur because of large SOC effects among low-lying states in such heavy metal-containing compounds. The minimum-energy crossing (MEX) point between the lowest quartet and sextet states is proved to be energetically and geometrically close to the transition state for the dissociation reaction on the potential energy surface of the lowest spin-mixed state. The MEX point (C_2 symmetry) was estimated to be 9184 cm^{-1} (26.3 kcal/mol) higher than the $^4A_2$ state in D_{2d} symmetry at the MRMP2 level of theory. After inclusion of SOC effects, an energy maximum on the lowest spin-mixed state appears near the MEX point and is recognized as the transition state for the dissociation reaction to ReH_2+H_2. The energy barrier for the dissociation, evaluated to be MEX in the adiabatic picture, was calculated to be 5643 cm^{-1} (16.1 kcal/mol) on the lowest spin-mixed state when SOC effects were estimated at the MCSCF level of theory. © *2010 American Institute of Physics*. [doi:10.1063/1.3495680]

I. INTRODUCTION

Recently, much attention has been paid to relativistic effects in molecules in many theoretical studies.[1–3] Several research groups have solved two-component or even four-component Dirac equations of molecules[4–11] and reported interesting results. Most of the theoretical studies, however, employed nonrelativistic Schrödinger equations of molecules together with relativistic effective core potential (RECP) and/or model core potential approximations.[12–20] In these investigations, the spin-independent (scalar) parts (mass-velocity and Darwin terms) of the relativistic effects are considered to be included in the core potentials and the spin-dependent parts (spin-orbit and spin-spin couplings) are described as a perturbation after orbital and geometrical optimizations.

In the series of studies in our research project, spin-orbit coupling (SOC) effects in chemical reactions have been explored since SOCs can explain electronic transitions between states of different spin-multiplicities, the so-called intersystem crossing or spin-forbidden reaction. Until now, potential energy curves of low-lying (spin-mixed) states were calculated for monohydrides of transition elements[21] and SOC effects were analyzed on dissociation potential energy curves, in which the one-electron approximation or effective nuclear charge (Z_{eff}) method was used for the Breit–Pauli Hamiltonian.[3,22] The calculated results have been reported for monohydrides of groups 3–7 transition elements.[21] This method has also been applied to investigation of the stabilities of dihydrides and tetrahydrides of third-row transition elements.[23,24] For applying SOC calculations to larger molecules, it would be useful to evaluate the reliability and usefulness of Z_{eff} approximation and to accumulate basic data on SOC effects in small molecules. Recently, it was successful to explain the phosphorescent processes in Pt and Ir complexes by using our computational methods.[25,26] These complexes are known to be the parent molecules of organic electroluminescence (EL) compounds or organic light-

a)Author to whom correspondence should be addressed. Electronic mail: shiro@c.s.osakafu-u.ac.jp.

 © 2010 American Institute of Physics

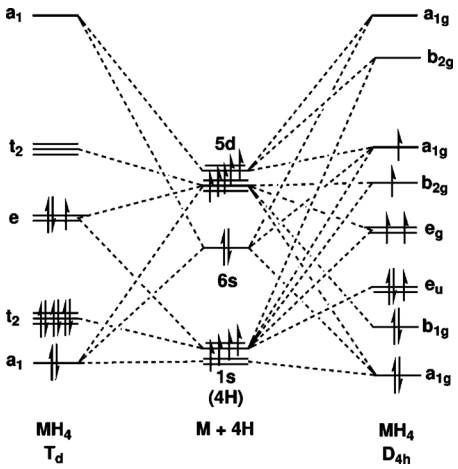

FIG. 1. Orbital correlation diagram. Electron occupations correspond to the main configuration of the ground states at the T_d and D_{4h} structures in Re H_4 (M=Re).

emitting diodes. The derivatives of these complexes are now under investigation in order to adjust wavelengths of phosphorescent spectra for the design of more effective EL compounds in industrial developments. Although the SBKJC basis sets are comparatively small and further investigation using larger basis sets may need to be performed, our theoretical investigations using the SBKJC basis sets provided reasonable explanations so far.

As for tetrahydrides of third-row transition elements, interesting results have been reported in our previous paper;[24] the T_d structures of HfH_4, TaH_4, WH_4, and OsH_4 were found to be explicitly lower in energy than the corresponding dissociation limits, MH_2+H_2 or $M+2H_2$ (M=third-row transition elements). The T_d structures are the most stable in HfH_4 and OsH_4 since the lowest states (ground states) have closed-shell electronic structures (Fig. 1),

$$HfH_4(^1A_1):(\text{core})(5s)^2(5p)^6(a_1)^2(t_2)^6,$$

$$OsH_4(^1A_1):(\text{core})(5s)^2(5p)^6(a_1)^2(t_2)^6(e)^4.$$

TaH_4 (^2E) and WH_4 ($^3A_2$) have singly occupied nonbonding degenerate orbitals and, as a result, are considered to be relatively stable. When attention is paid to geometrical deformation from the D_{4h} structure to the T_d structure, the spin-multiplicity of the lowest state is maintained along the deformation paths in HfH_4 (singlet), TaH_4 (doublet), and WH_4 (triplet). On the other hand, in OsH_4, the lowest state is quintet at the D_{4h} structure, while its T_d structure has a stable singlet ground state (see Table I). Therefore, as long as only the lowest state is considered along the deformation path from the D_{4h} structure to the T_d structure, it is not necessary to consider interaction among the states of different spin-multiplicities in HfH_4, TaH_4, and WH_4, but the interaction among the states of different spin-multiplicities, namely, SOC effects, must be taken into account in OsH_4 for the purpose of exploring the deformation potential energy surface from the D_{4h} structure to the T_d structure, as described in our previous paper.[24]

High symmetry species with multiple unpaired electrons can lower its symmetry through the Jahn–Teller effect. The lowest state at the T_d structure of ReH_4 has three electrons in the doubly degenerate nonbonding orbitals, characterized as "e" irreducible representation, and thus its state symmetry is ^2E (Fig. 1),

$$ReH_4(^2E):(\text{core})(5s)^2(5p)^6(a_1)^2(t_2)^6(e)^3.$$

Accordingly, this T_d structure can be distorted into a D_{2d} structure by Jahn–Teller effects. In fact, Wang and Andrews[27] reported the $^2A_1$ state in ReH_4 with a D_{2d} structure. They also reported that ReH_4 is more stable than the dissociation limit by 26 kcal/mol based on the IR spectra and their density functional theory (DFT) calculations. Unfortunately, this result does not match well with our previous result that the energy difference between the lowest state at the T_d structure and its dissociation limit ReH_2+H_2 is rather small.[24] Although there are only small amount of rhenium compounds in nature, it has been reported that these compounds can be used as effective catalyzes for the activation of C–H bonds[28,29] as well as hydrogen strorages.[27]

In the light of ReH_4 possibly possessing the Jahn–Teller distortion, along with large SOC, it would be interesting for us to explore further the potential energy surface of ReH_4. This paper focuses on SOC effects on the stability of ReH_4. Computational methods are described in detail in the next section. In the third section, the deformation paths of ReH_4

AQ: #3

AQ: #4

AQ: #16

TABLE I. Comparison of the stabilities of MH_4, MH_2+H_2, and $M+2H_2$, where M is a transition element in the third series. The geometrical structures were optimized using the MCSCF/SBKJC method and their relative energies were refined at the MCSCF+MRMP2/SBKJC+p level of theory.

	T_d		D_{4h}		MH_2+H_2		$M+2H_2$	
LaH_4	51.0	$^2T_2$	60.8	^2E_u	0.0	$^2A_1$	12.3	^2D
HfH_4	−42.6	$^1A_1$	14.5	$^1A_{1g}$	0.0	$^1A_1$	24.1	^3F
TaH_4	−40.0	^2E	11.1	$^2A_{1g}$	0.0	$^4A_2$	8.0	^4F
WH_4	−24.6	$^3A_2$	54.5	^3E_g	0.0	$^5B_2$	15.1	^7S
ReH_4	−5.8	^2E	44.8	^6E_u	0.0	$^6\Sigma_g^+$	−2.7	^6S
OsH_4	−42.8	$^1A_1$	15.9	$^5B_{2g}$	0.0	$^3B_1$	5.4	^5D
IrH_4	−0.2	$^2T_2$	77.1	$^2A_{2u}$	0.0	$^2A_1$	32.2	^4F
PtH_4	61.3	$^3T_2$	74.4	^3E_u	0.0	$^1A_1$	54.1	^3D
							62.2	^3F
AuH_4	70.1	$^4A_1$	34.6	^2E_u	0.0	$^2B_2$	−9.3	^2S
HgH_4	132.7	^1E	48.0	$^1A_{1g}$	0.0	$^1\Sigma_g^+$	−26.1	^1S

within an adiabatic picture are first discussed, and then, the dissociation path from the most stable structure of ReH_4 is carefully explored and the energy barrier for the dissociation is estimated. It is revealed that SOC effects play essential roles in the dissociation reaction of ReH_4.

II. METHODS OF CALCULATION

Optimization of the stationary structures for ReH_4 was performed using the full optimized reaction space multiconfiguration self-consistent field (MCSCF) method with the SBKJC RECPs and the associated basis sets for Re atom[12] and the 31G basis set for H atoms, where they are augmented by a set of polarization functions, respectively.[30] The MCSCF active space includes 13 orbitals correlating to the 5d, 6s, and 6p orbitals of Re atom and 1s orbitals of H atoms in the dissociation limit, and 11 electrons are included in this MCSCF active space. The relative energies of the stationary structures were recalculated by using the second-order multireference Møller–Plesset perturbation (MRMP2) method,[31] where the results were excluded when intruder states appeared.

The SOC integrals at all points on the potential energy surfaces of low-lying states were computed using MCSCF/SBKJC+p optimized orbitals by the state-averaged technique with equal weights (see discussion below).[32] Since SBKJC belongs to RECP basis sets, one-electron approximation [or effective nuclear charge (Z_{eff}) approximation] should be employed for estimation of SOC effects.[22] In order to keep the size of SOC matrices computationally tractable, adiabatic states whose energies are lower in energy than a specific upper limit of energies were included in SOC matrices.[33]

All of these calculations were carried out using the GAMESS suite of program codes.[34]

III. RESULTS AND DISCUSSION

A. Jahn–Teller and pseudo-Jahn–Teller deformation

In order to systematically explore the potential energy surface of the lowest state in ReH_4, Jahn–Teller and pseudo-Jahn–Teller theories were applied. The highest symmetries for tetrahydrides are D_{4h} and T_d, and the lowest states (ground states) in ReH_4 are found to be ^6E_u and ^2E at the D_{4h} and T_d structures, respectively, at the MRMP2 level of theory (see Table I).[24]

1. D_{4h} structure

The D_{4h} structure has ^6E_u ground state and is remarkably higher in energy than the T_d structure (Fig. 1). Unfortunately, normal-mode analysis could not be performed for such a doubly degenerate state, but single-point energy calculations at the distorted geometries along appropriate nuclear displacements suggest that this state has two imaginary frequencies for b_{2g} and e_u modes. The b_{2g} geometrical deformation is explained by Jahn–Teller effects as follows. Based on Taylor expansion of an electronic Hamiltonian in the power series of a nuclear displacement Q at the D_{4h} structure ($Q=0$), the total energy $E_0(Q)$ of the lowest state at a displaced structure can be expanded into

$$E_0(Q) = \langle 0|H(Q)|0\rangle = \left\langle 0 \left| H(0) + \left(\frac{\partial H}{\partial Q}\right)_0 Q \right.\right. \tag{189}$$

$$\left.\left. + \frac{1}{2}\left(\frac{\partial^2 H}{\partial Q^2}\right)_0 Q^2 + \cdots \right| 0 \right\rangle, \tag{190}$$

$$= \langle 0|H(0)|0\rangle + \left\langle 0 \left| \left(\frac{\partial H}{\partial Q}\right)_0 \right| 0 \right\rangle Q \tag{191}$$

$$+ \frac{1}{2}\left\langle 0 \left| \left(\frac{\partial^2 H}{\partial Q^2}\right)_0 \right| 0 \right\rangle Q^2 + \cdots. \tag{192}$$

When $|0\rangle \approx |^6E_u\rangle$ is used, Q (or $\partial H/\partial Q$) needs to belong to the irreducible representation provided by the product of E_u (bra) and E_u (ket) in order to obtain Jahn–Teller stabilization $\langle 0|(\partial H/\partial Q)_0|0\rangle < 0$. The product of state symmetry (^6E_u) provides four irreducible representations,

$$E_u \otimes E_u = a_{1g} \oplus a_{2g} \oplus b_{1g} \oplus b_{2g}. \tag{198}$$

A totally symmetric a_{1g} motion does not provide any energy lowering or any geometrical deformation since the geometry has been optimized within D_{4h} symmetry. There is no a_{2g} motion for this molecule. The b_{1g} and b_{2g} motions provide rhombic and rectangular structures [see Fig. 2(a)]. Geometrical optimizations with the constraint of D_{2h} symmetry prove that on the lowest sextet potential energy surface, no stable rhombic structures exist while two identical rectangular structures have been found. The lowest states at the two rectangular structures (D_{2h}) are $^6B_{2u}$ and $^6B_{3u}$, which are completely identical except for the 90° rotation around the C_2 axis perpendicular to the molecular plane.[35] These rectangular structures have one imaginary-frequency mode, b_{3u} (or b_{2u}), which is described as pseudo-Jahn–Teller distortion along this mode to produce a planar C_{2v} structure. Geometry optimization with the constraint of planar C_{2v} symmetry provides the dissociation to $ReH_2(^6\Sigma_g^+) + H_2(^1\Sigma_g^+)$.

As mentioned above, another geometrical deformation of the D_{4h} structure needs to be considered: a geometrical displacement along the e_u motion derives two identical planar C_{2v} structures. These deformations can be explained by pseudo-Jahn–Teller theory. The lowest state at the C_{2v} structure is $^6A_1$ and geometry optimization for this state provides the dissociation to linear $ReH_2(^6\Sigma_g^+) + H_2(^1\Sigma_g^+)$. Thus, no energy minima are located on the potential energy surface of the lowest sextet state when a planar structure is chosen as the initial geometry. We also examined the displacements along out-of-plane modes, but no energy lowering was obtained on the potential energy surface of the lowest sextet state.

2. T_d structure

The lowest state (ground state) at the optimized T_d structure is ^2E as described above. The present MCSCF calculations suggest that the T_d structure on the potential energy surface of the lowest state is slightly deformed into two different D_{2d} structures and that the lowest states of these D_{2d}

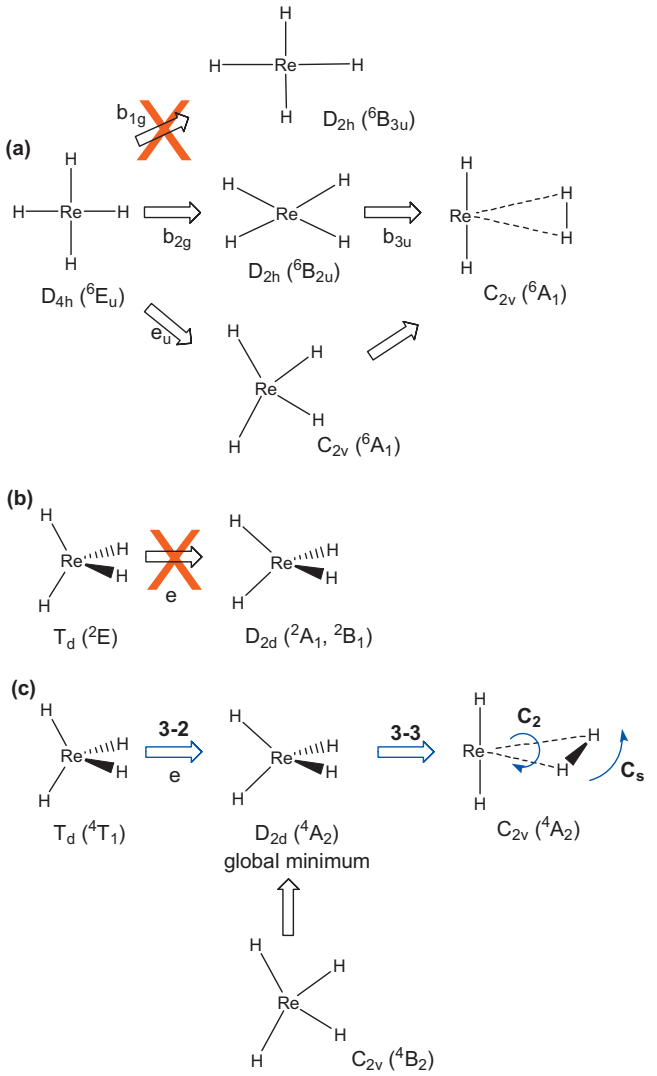

FIG. 2. Geometrical deformation paths on the potential energy surfaces of (a) the lowest sextet state, (b) the lowest doublet state, and (c) the lowest quartet state. The total energy explicitly rises along the red-crossed paths.

structures are $^2A_1$ and $^2B_1$, respectively, the $^2B_1$ state being slightly lower in energy than the $^2A_1$ state [see Fig. 2(b)]. However, dynamic correlation effects estimated by using the MRMP2 method make the T_d structure (^2E state) slightly lower than the D_{2d} ones ($^2A_1$ and $^2B_1$ states) and indicate that no Jahn–Teller distortion occurs in this ^2E state at the T_d structure.

As shown in Table II, the ^2E state at the T_d structure is the most stable on the potential energy surface of the lowest doublet state. This state is apparently lower in energy than the lowest doublet state in the dissociation limit. However, the ground state in the dissociation limit is $ReH_2(^6\Sigma_g^+)$ $+H_2(^1\Sigma_g^+)$ and is lower in energy than the T_d structure (^2E) by 12.9 kcal/mol at the MCSCF level of theory. Again, dynamic correlation effects estimated by using the MRMP2 method make the T_d structure lower in energy than the ground state in the dissociation limit by 6.7 kcal/mol. Further investigation suggested that the other stationary structures on the lowest doublet state are apparently higher in energy than the T_d structure, as shown in Table II.

3. Lowest quartet state

The potential energy surfaces of the lowest doublet and sextet states in the target molecule were explored in the previous two sections. It is necessary to examine the potential energy surface of the lowest quartet state of this molecule as well. The lowest quartet states are relatively low-lying in energy at both D_{4h} and T_d structures, as shown in Table II, in comparison with their ground states.

Two relatively stable stationary structures were found on the lowest quartet potential energy surface, $D_{2d}(^4A_2)$ and planar $C_{2v}(^4B_2)$ structures [see Fig. 2(c)]. The $^4B_2$ state at the planar C_{2v} structure is higher in energy than the most stable doublet state (^2E at the T_d structure) by only 1.6 kcal/mol (MRMP2). The planar $C_{2v}(^4B_2)$ structure has one imaginary frequency and its motion is out-of-plane. Geometry optimization starting at a displaced structure along this out-of-plane motion finally provides the $D_{2d}(^4A_2)$ structure. The $^4A_2$ state at the D_{2d} structure is lower in energy than the most stable doublet state (^2E at the T_d structure) by 2.1 kcal/mol (MRMP2). Even though the $D_{2d}(^4A_2)$ structure also has one imaginary frequency at the MCSCF level of theory, it is found after the inclusion of dynamic correlation effects (MRMP2) that the deformation to a nonsymmetrical structure is an artifact. Thus, it can be concluded that the global energy minimum for ReH_4 is the $D_{2d}(^4A_2)$ structure and it is lower in energy than the dissociation limit by 8.8 kcal/mol at the MRMP2 level of theory (see Table II). This conclusion is consistent with the previous experimental suggestion reported by Wang and Andrews.[27]

B. Deformation paths

Since strong SOC effects are expected in such heavy metal compounds, it would be interesting to investigate potential energy surfaces of low-lying states between the stable structures of different spin-multiplicities. In the present investigation, one of H–Re–H angles is taken as the reaction coordinate from the T_d structure (^2E) to the D_{2d} structure ($^4A_2$), and D_{2d} symmetry is maintained along the whole range of the reaction path [see 3-2 in Fig. 2(c)].

The lowest state (^2E) at the T_d structure is split into $^2A_1$ and $^2B_1$, when the structure is deformed into a D_{2d} structure, while the lowest state ($^4A_2$) at the D_{2d} structure correlates with the lowest quartet state ($^4T_1$) at the T_d structure. Since the $^4T_1$ state is split into $^4A_2$ and ^4E states by geometrical deformation of the T_d structure to a D_{2d} structure, state averaging was performed over four states, the lowest $^2A_1$, $^2B_1$, $^4A_2$, and ^4E states. Figure 3 shows potential energy curves of low-lying adiabatic and spin-mixed states obtained at the four-state-averaged MCSCF level of theory with equal weights. Although the $^2B_1$ state becomes slightly stable at the beginning of displacement from the T_d structure, the potential energy curves of both doublet states ($^2B_1$ and $^2A_1$) finally increase [Fig. 3(a)]. The potential energy curve of the lowest E state increases immediately, while that of the lowest $^4A_2$ state rapidly decreases, and this state becomes the lowest state in the vicinity of the stable D_{2d} structure. Since the spin-multiplicities of the lowest states at the T_d and D_{2d}

AQ: #17

TABLE II. Stationary geometries of ReH_4. The geometrical structures were optimized using the MCSCF/SBKJC+p method and their relative energies were refined at the MCSCF+MRMP2/SBKJC+p level of theory.

Structure	Symmetry	State	Re–H (Å)	H–Re–H (deg)	MCSCF (kcal/mol)	MRMP2 (kcal/mol)	Imaginary frequency[a] (cm^{-1})
Planar	D_{4h}	^6E_u	1.801	90.0	55.1	44.6	
		^4E_u	1.828	90.0	57.2	48.4	
		^2E_u	1.779	90.0	97.6	91.9	
		$^2A_{1g}$	1.781	90.0	96.4	93.4	i2512
							i2255
							i1138
							(e)
	C_{2v}	$^4B_2$	1.761	63.7	**4.9**	**−5.1**	i109
			1.667	154.7			
		$^2A_1$	1.643	57.5	42.6	33.8	i2133
			1.770	156.4			i441
Tetrahedral	T_d	^2E	1.671	109.5	12.9	−6.7	
		$^4T_1$	1.714	109.5	24.0	8.4	
	D_{2d}	$^4A_2$	1.716	73.5	**5.5**	**−8.8**	i2633
				130.0			(e)
		$^2B_1$	1.671	107.47	3.2	**-5.4**	p.d.
				113.55			
Rhombic	D_{2h}	$^6B_{2u}$	1.798	90.0	53.7	45.6	i1723
			1.802				i751
Rectangular	D_{2h}	$^6B_{2u}$	1.781	57.0	40.8	29.1	i891
				123.0			
Square pyramidal	C_{4v}	$^2A_1$	1.646	73.3	17.0	5.8	i2201
		^4E	1.707	79.5	24.1	9.2	i2011
Distorted-pyramidal	C_{2v}	$^2A_1$	1.641	75.9	15.2	6.0	p.d.
Re $H_2(^6\Sigma_g^+)+H_2(^1\Sigma_g^+)$			1.820	180.0	0	0	
Re $H_2(^4\Pi_g)+H_2(^1\Sigma_g^+)$			(1.820)	180.0	50.8	47.2	
Re $H_2(^2\Sigma_g^+)+H_2(^1\Sigma_g^+)$			(1.820)	180.0	74.9	66.7	
$Re(^6S)+2H_2(^1\Sigma_g^+)$					−5.4	−2.8	

[a]"p.d." means "positive definite."

structures are different, their potential energy curves of the doublet and quartet states run across each other within an adiabatic picture, as shown in Fig. 3(a).

When SOC effects are considered within D_{2d} symmetry, both $^2A_1$ and $^2B_1$ states belong to $E_{1/2}$ in the double-group representation, while the $^4A_2$ state is split into $E_{1/2}$ and $E_{3/2}$.

Accordingly, avoided crossings occur among the potential energy curves of $E_{1/2}$ states and among those of $E_{3/2}$ states. Because of the large SOC integrals in such heavy metal compounds, large energy splittings among spin-mixed states make the lowest spin-mixed state considerably lowered.

This is the reason why the potential energy curve of the lowest spin-mixed state monotonically decreases along the deformation path from the T_d structure to the D_{2d} structure [Fig. 3(b)]. This result is explained as follows: the lowest $E_{1/2}$ state principally has a $^2B_1$ adiabatic component near the T_d structure, while it mainly has a $^4A_2$ adiabatic component after the crossing (H–Re–H $< 100°$) between the potential energy curves of the adiabatic $^2B_1$ and $^4A_2$ states. Thus, as a result, no energy barrier is obtained along the geometrical deformation from the T_d structure to the D_{2d} structure in a relativistic picture.

C. Dissociation paths into ReH_2+H_2

As described in Sec. III A, the lowest state (^6E_u) at the D_{4h} structure is very high in energy and no energy barrier is found along the C_{2v} dissociation paths starting at the D_{4h} structure to the ground state $ReH_2(^6\Sigma_g^+)+H_2(^1\Sigma_g^+)$ in the dissociation limit. On the other hand, the global minimum has a D_{2d} structure and its lowest state is not sextet but quartet ($^4A_2$), as discussed in the previous section. In such heavy metal compounds, it is necessary to consider the SOC effects among low-lying quartet and sextet states in order to obtain reasonable dissociation paths. Note that the dissociation limit ReH_3+H, as well as $Re+2H_2$, is apparently higher in energy than $ReH_2(^6\Sigma_g^+)+H_2(^1\Sigma_g^+)$.

AQ: #7

AQ: #8

When the reaction coordinate is assumed to be the distance between the Re atom and the geometrical center of the leaving hydrogen molecule and molecular symmetry (C_{2v}) is maintained along the whole range of the dissociation path [see 3-3 in Fig. 2(c)], the potential energy curves of low-lying states were calculated, as shown in Fig. 4, where the horizontal axis in this figure is taken as the distance between the Re atom and one of the leaving hydrogen atoms. State averaging was performed over two states, the lowest $^4A_2$ state (lowest state at the D_{2d} structure) and the lowest $^6A_1$ state (ground state in the dissociation limit) along the C_{2v}

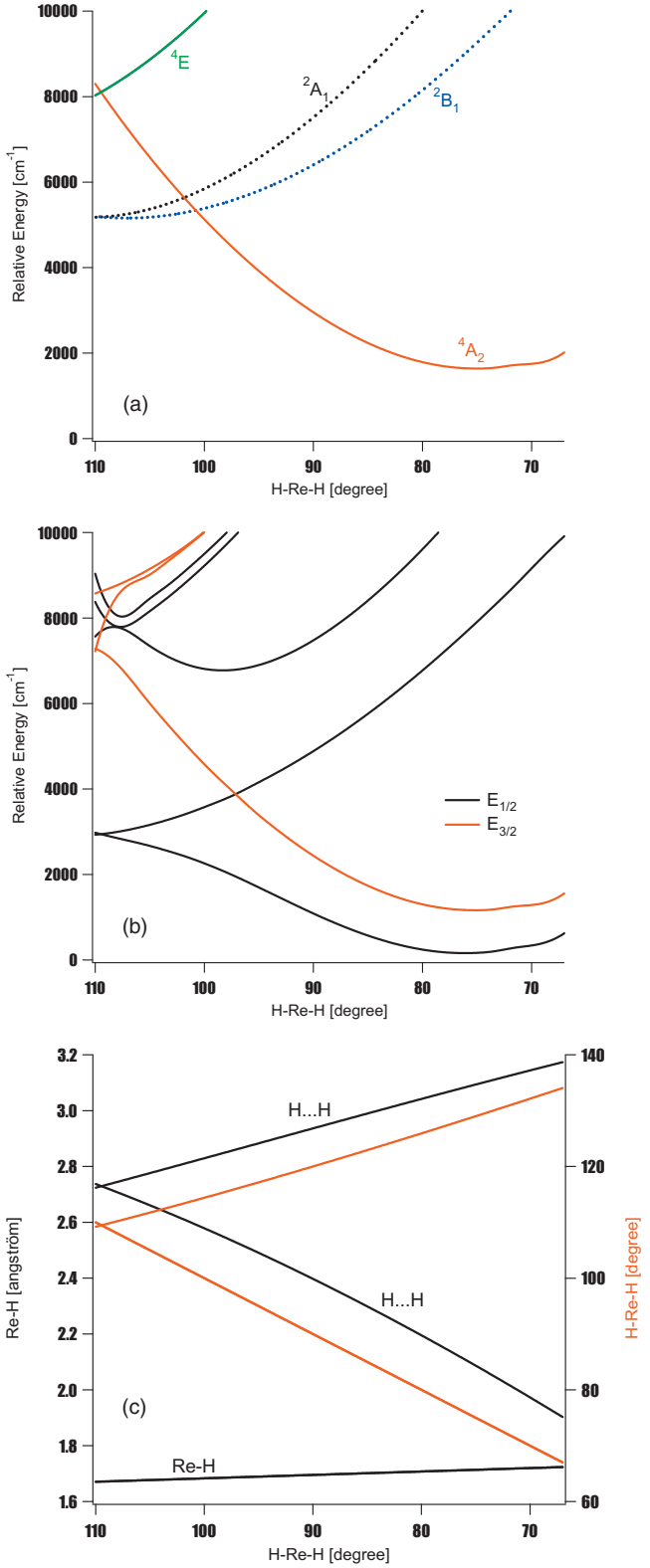

FIG. 3. Potential energy curves of (a) low-lying adiabatic states obtained using four-state averaged MCSCF methods with equal weights and (b) low-lying spin-mixed states obtained after inclusion of SOC effects. (c) Geometrical changes along the C_{2v} dissociation path (see the text).

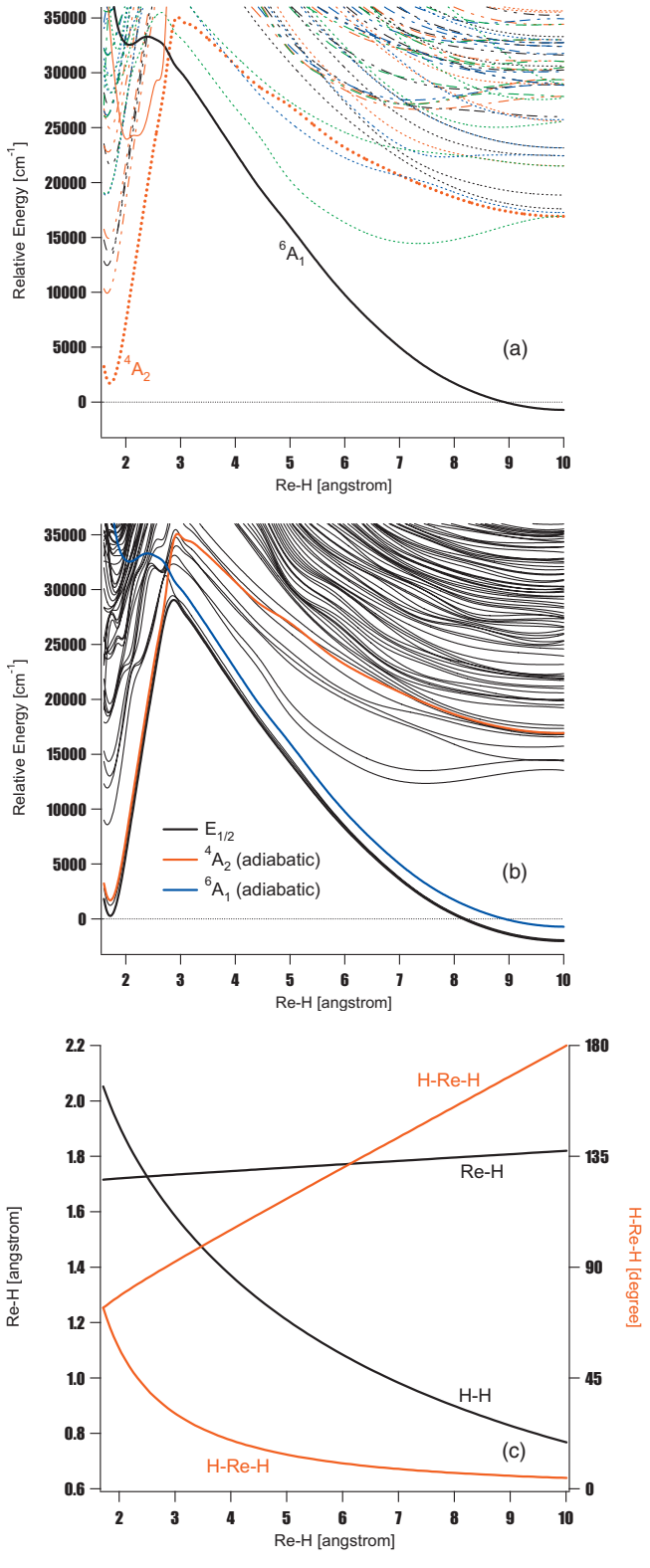

FIG. 4. Potential energy curves of (a) low-lying adiabatic states obtained using four-state averaged MCSCF methods with equal weights and (b) low-lying spin-mixed states obtained after inclusion of SOC effects. (c) Geometrical changes along the C_{2v} dissociation path (see the text).

dissociation path. Since it is meaningless for the geometry to be optimized for the lowest quartet or the lowest sextet state at each point of the dissociation path, the linear dissociation path is assumed. (Optimized geometry will be reported in the following discussion.)

As shown in Fig. 4(a), the potential energy curve of the lowest quartet state rapidly rises as the Re–H distance increases. The energy maximum appears at the Re–H distance of 2.944 Å on the lowest quartet state ($^4A_2$). The energy barrier on the lowest quartet state for the dissociation reac-

tion is estimated to be very high, partly because geometry optimization has not yet been performed. Within an adiabatic picture, this quartet state correlates not to the ground state, $ReH_2(^6\Sigma_g^+)+H_2(^1\Sigma_g^+)$, but to one of the excited states, $ReH_2(^4\Pi)+H_2(^1\Sigma_g^+)$, in the dissociation limit. On the other hand, the lowest sextet state ($^6A_1$) holds a local minimum at around 2 Å and peaked at 2.5 Å; subsequently, the energy remarkably decreases as the Re–H distance increases and dissociates into the ground state $ReH_2(^6\Sigma_g^+)+H_2(^1\Sigma_g^+)$ in the dissociation limit.

When describing the dissociation reaction within an adiabatic picture, the D_{2d} structure ($^4A_2$) should overcome the energy maximum on the potential energy surface of the lowest quartet and then be deactivated into the ground state, or it should be promoted to the lowest sextet state first, and then the dissociation reaction is accelerated on the repulsive potential energy surface of the lowest sextet state. The main configurations of the lowest quartet and sextet states within C_{2v} symmetry are

$$^4A_2:(\text{core})(1a_1)^2(2a_1)^2(1b_2)^2(1b_1)^2(1a_2)^1(3a_1)^1(4a_1)^1$$

and

$$^6A_1:(\text{core})(1a_1)^2(2a_1)^2(1b_2)^2(1b_1)^2(1a_2)^1(3a_1)^1(4a_1)^1(2b_2)^1.$$

The transition from the $^4A_2$ state to the $^6A_1$ state corresponds principally to the transition from the $1b_1$ orbital to the $2b_2$ orbital. However, since large SOCs occur between the lowest quartet and sextet states in such heavy metal compounds, it can be easily understood that the crossing point between the potential energy curves of the lowest quartet and sextet states is energetically and geometrically close to a transition state on the potential energy surface of the lowest spin-mixed state after inclusion of SOC effects. This is explained as follows: the lowest quartet state $^4A_2$ and the lowest state $^6A_1$ split into two and three spin-mixed states because of SOC effects, respectively, and all these spin-mixed states belong to $E_{1/2}$ in C_{2v} double-group representation. Accordingly, avoided crossings occur among the potential energy curves of these spin-mixed states, as shown in Fig. 4(b).

The potential crossing point between the lowest quartet and sextet states appears at the Re–H distances of 2.784 Å [see Fig. 4(a)] and is apparently lower in energy than the energy maximum on the potential energy curve of the lowest quartet state. The energy difference between this crossing point and the reactant [namely, the stable D_{2d} structure ($^4A_2$)] is calculated to be 29 071 cm^{-1} (83.1 kcal/mol) at the MCSCF level of theory. When the SO effects are included, the energy maximum on the potential energy curve of the lowest spin-mixed state appears at the Re–H distances of 2.875 Å and it is higher in energy than the reactant by 26 394 cm^{-1} (75.5 kcal/mol). As mentioned above, the geometry has not yet been optimized for either the lowest quartet state or the lowest sextet state, so that the energy barrier is apparently overestimated. Unfortunately, geometry optimization cannot be performed after inclusion of SOC effects at the present stage, but the minimum-energy crossing (MEX) point[36–38] between the lowest quartet and sextet states must be energetically and geometrically close to the true transition state on the potential energy surface of the lowest spin-mixed state, as discussed above.

First, the MEX point has been searched within C_{2v} symmetry. The geometry at the C_{2v} MEX point is found to have Re–H bonds of 1.762 Å with the H–Re–H angle of 86.1° for the ReH_2 moiety and the Re–H distances of 2.698 Å with the H–H distance of 1.430 Å for the leaving hydrogen molecule. The energy difference between the MEX point and the reactant is calculated to be 23 539 cm^{-1} (67.3 kcal/mol) with state-specific MCSCF calculations having been performed for both lowest quartet and sextet states. The MRMP2 calculations raise this difference to 28 080 cm^{-1} (80.3 kcal/mol). Note that the reactant is lower in energy than the dissociation limit by 3442 cm^{-1} (9.8 kcal/mol) at the MRMP2 level of theory, as described in the previous section.

It is natural to consider that the geometrical deformation from the C_{2v} MEX point to a lower symmetry MEX point may provide a lower energy barrier obtained after inclusion of SOC effects. In the present investigation, MEX point searches were carried out using twisted (C_2) and bent (C_s) structures [see 3-3 in Fig. 2(c)]. The calculated results indicate that the geometrical deformation from the C_{2v} structure to a C_2 structure and to a C_s structure remarkably reduces the energy difference between the MEX point and the reactant to 6807 cm^{-1} (19.5 kcal/mol) for C_2 symmetry and to 9748 cm^{-1} (27.9 kcal/mol) for C_s symmetry. The results show that the C_2 path is more preferred for the dissociation. The geometry at the C_2 MEX point has Re–H bonds of 1.704 Å with the H–Re–H angle of 86.1° and Re–H distances of 2.169 Å with the H–H distance of 0.794 Å for the leaving hydrogen molecule. The twisted angle from the C_{2v} to C_2 structure is only 1.6°. The stabilization of the C_2 MEX point would be caused by the fact that the H–H distance is considerably shortened in comparison with that for the C_{2v} MEX point [Fig. 4(c)]. We also examined whether or not a lower C_1 MEX point exists, but no lower C_1 MEX point was found.

In order to confirm that there is no energy barrier between the C_2 MEX point and the reactant on the lowest quartet potential energy surface and between the C_2 MEX point and the dissociation limit $ReH_2(^6\Sigma_g^+)+H_2(^1\Sigma_g^+)$ on the lowest sextet potential energy surface, steepest descent paths starting at the C_2 MEX point were generated on the potential energy surfaces of both lowest quartet and sextet states. Figure 5(a) shows that no energy barrier exists for both paths from the C_2 MEX point to the reactant and to the dissociation limit. Note that Fig. 5(c) shows the dependency of the Re–H distances and the H–Re–H angle for the leaving hydrogen molecule on the reaction coordinate "s." As described above, after inclusion of SOC effects, avoided crossing occurs for the potential energy curves of the lowest two spin-mixed states ($E_{1/2}$) [see Fig. 5(b)], which originates from the quartet and sextet adiabatic states. In these calculations, instead of state-specific MCSCF methods, state averaging was performed over two states, the lowest $^4A_2$ and $^6A_1$ states, so that the crossing point between these states is about 1800 cm^{-1} (5.1 kcal/mol) higher in energy that obtained by using state-specific MCSCF methods. After inclusion of

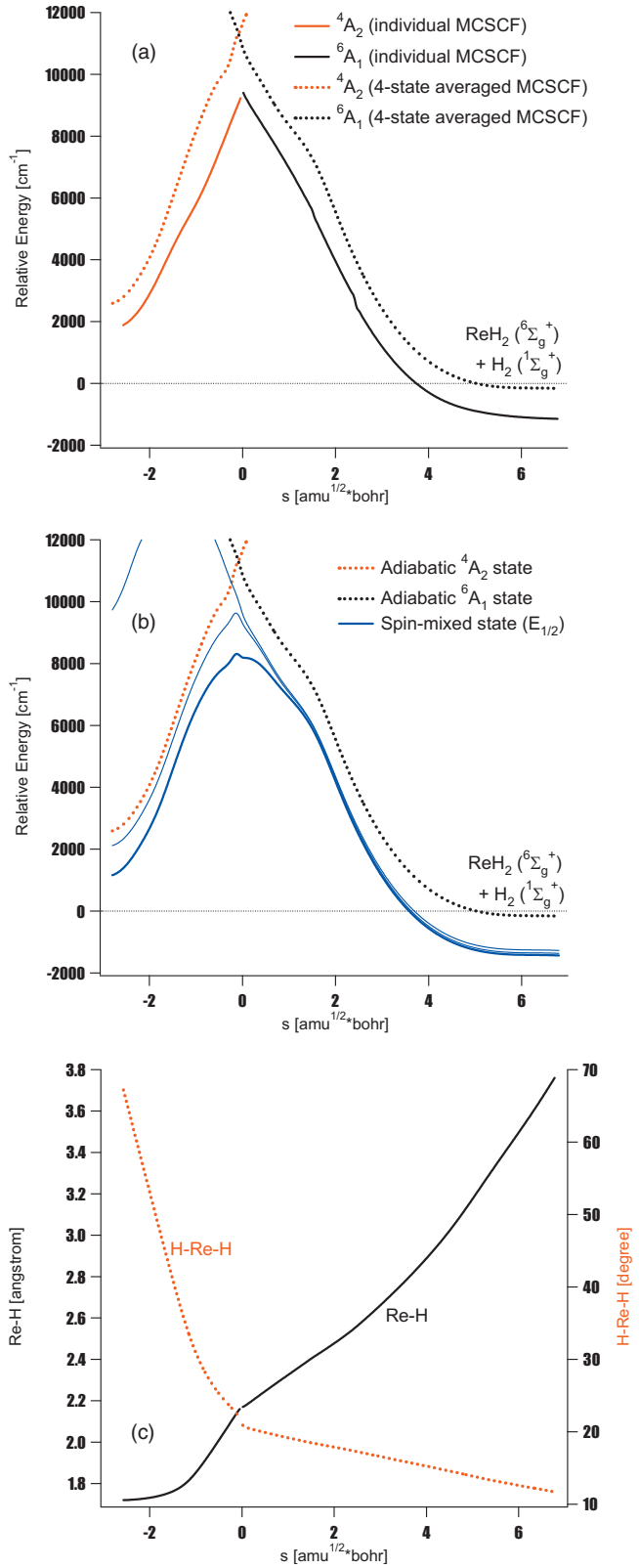

FIG. 5. Potential energy curves of (a) lowest quartet (red) and lowest sextet (black) states obtained using state-specific MCSCF methods (solid lines) and four-state averaged MCSCF methods with equal weights (broken lines). (b) Low-lying spin-mixed states (blue) obtained after inclusion of SOC effects. (c) Re–H distance and H–Re–H angle for the leaving hydrogen molecule along the minimum-energy paths on the lowest quartet (negative **s**) and sextet (positive **s**) states.

SOC effects [see Fig. 5(b)], the energy maximum on the lowest spin-mixed state appears near the C_2 MEX point and it is the transition state for the dissociation reaction. The energy barrier is calculated to be 5643 cm^{-1} (16.1 kcal/mol) on the potential energy surface of this lowest spin-mixed state. Note that on the basis of our experiences described in the previous sections, the state-specific MCSCF method makes this barrier smaller, but MRMP2 calculations make it larger because of larger effects of dynamic correlation in the reactant (see Table II). AQ: #10

IV. SUMMARY

The potential energy surface of low-lying states in rhenium tetrahydride was explored by using the MCSCF method together with the SBKJC basis sets augmented by a set of *f* functions on rhenium atom and by a set of *p* functions on hydrogen atoms, followed by SOC calculations. The relative energies at the stationary geometries were recalculated by the MRMP2 method.

The most stable structure of ReH_4 has a D_{2d} structure and its ground state is $^4A_2$. It was found that this is lower in energy than the dissociation limit, $ReH_2(^6\Sigma_g^+)+H_2(^1\Sigma_g^+)$, by 8.8 kcal/mol after dynamic correlation effects are considered by using the MRMP2 method. This is consistent with previous results reported by Andrews *et al.*[27] Since the spin-multiplicities of the lowest states are different, the dissociation reaction of ReH_4 cannot occur without electronic transition from the lowest quartet state to the lowest sextet state. This transition can easily occur because of the strong SOC effects among low-lying states in such heavy metal compounds. First, the C_{2v} MEX point was located and the geometrical deformations to C_2 and C_s symmetries were examined. Finally, it was revealed that the C_2 MEX point is higher in energy than the reactant with D_{2d} structure ($^4A_2$) by 6807 cm^{-1} (19.5 kcal/mol) at the MCSCF level of theory and by 9184 cm^{-1} (26.3 kcal/mol) at the MRMP2 level of theory. After inclusion of SOC effects, the potential energy surfaces of the lowest quartet and sextet states avoid across each other and an energy maximum appears on the potential energy surface of the lowest spin-mixed state [see Fig. 5(b)]. This energy maximum is recognized as the transition state for the dissociation reaction, $ReH_4 \rightarrow ReH_2+H_2$.

ACKNOWLEDGMENTS

This work was partly supported by a Grant-in-Aid for Scientific Research on Priority Areas "Molecular Theory for Real Systems" from the MEXT of the Japanese Government (Grant Nos. 19029040 and 20038042).

[1] B. A. Heß, C. M. Marian, and S. D. Peyerimhoff, in *Modern Electronic Structure Theory, Part I*, edited by D. R. Yarkony (World Scientific, Singapore, 1995), p. 152; C. M. Marian, in *Problem Solving in Computational Molecular Science*, edited by S. Wilson and G. H. F. Diercksen (Kluwer Academic, Dordrecht, 1997), p. 291; C. M. Marian, in *Reviews in Computational Chemistry*, edited by K. B. Lipowitz and D. B. Boyd (Wiley-VCH, New York, 2001), Vol. 17, p. 99. AQ: #11
[2] K. Balasubramanian, *Relativistic Effects in Chemistry, Part A and B* (Wiley, New York, 1997).
[3] D. G. Fedorov, S. Koseki, M. W. Schmidt, and M. S. Gordon, Int. Rev. Phys. Chem. **22**, 551 (2003); D. G. Fedorov, M. W. Schmidt, S. Koseki,

and M. S. Gordon, *Recent Advances in Relativistic Molecular Theory* (World Scientific, Singapore, 2004), Vol. 5, p. 107.
[4] L. L. Foldy and S. A. Wouthhuysen, Phys. Rev. **78**, 29 (1950).
[5] M. Douglas and N. M. Kroll, Ann. Phys. **82**, 89 (1974).
[6] K. G. Dyall, I. P. Grant, C. T. Johnson, F. A. Parpia, and E. P. Plummer, Comput. Phys. Commun. **55**, 425 (1989).
[7] T. Yanai, H. Nakano, T. Nakajima, T. Tsuneda, S. Hirata, Y. Kawashima, T. Nakao, M. Kamiya, H. Sekino, and K. Hirao, Lect. Notes Comput. Sci. **2660**, 84 (2003) and references therein.
[8] M. Reiher and A. Wolf, J. Chem. Phys. **121**, 2037 (2004); M. Reiher and A. Wolf, *ibid.* **121**, 10945 (2004); A. Wolf and M. Reiher, *ibid.* **124**, 064102 (2006); A. Wolf and M. Reiher, *ibid.* **124**, 064103 (2006).
[9] P. Krekora, Q. Su, and R. Grobe, Phys. Rev. A **70**, 054101 (2004).
[10] D. Kędziera, J. Chem. Phys. **123**, 074109 (2005).
[11] Y. Watanabe, H. Tatewaki, and T. Koga, J. Comput. Chem. **27**, 48 (2006); T. Tsuchiya, M. Abe, T. Nakajima, and K. Hirao, J. Chem. Phys. **115**, 4463 (2001).
[12] W. J. Stevens and M. Krauss, Chem. Phys. Lett. **86**, 320 (1982); W. J. Stevens, H. Basch, and M. Krauss, J. Chem. Phys. **81**, 6026 (1984); W. J. Stevens, H. Basch, M. Krauss, and P. Jasien, Can. J. Chem. **70**, 612 (1992); T. R. Cundari and W. J. Stevens, J. Chem. Phys. **98**, 5555 (1993).
[13] P. J. Hay and W. R. Wadt, J. Chem. Phys. **82**, 270 (1985); W. R. Wadt and P. J. Hay, *ibid.* **82**, 284 (1985); P. J. Hay and W. R. Wadt, *ibid.* **82**, 299 (1985).
[14] W. C. Ermler, R. B. Ross, and P. A. Christiansen, Adv. Quantum Chem. **19**, 139 (1988); R. B. Ross, J. M. Powers, T. Atashroo, W. C. Ermler, L. A. Lajohn, and P. A. Christiansen, J. Chem. Phys. **93**, 6654 (1990).
[15] W. Küchle, M. Dolg, H. Stoll, and H. Preuss, Mol. Phys. **74**, 1245 (1991); M. Kaupp, P. R. Schleyer, H. Stoll, and H. J. Preuss, J. Chem. Phys. **94**, 1360 (1991); A. Bergner, M. Dolg, W. Kuechle, H. Stoll, and H. Preuss, Mol. Phys. **80**, 1431 (1993); M. Dolg, H. Stoll, H. Preuss, and R. M. Pitzer, J. Phys. Chem. **97**, 5852 (1993).
[16] Y. Sakai, Y. E. Miyoshi, M. Klobukowski, and S. Huzinaga, J. Comput. Chem. **8**, 226 (1987); Y. Sakai, E. Miyoshi, M. Klobukowski, and S. Huzinaga, *ibid.* **8**, 256 (1987); Y. Sakai, E. Miyoshi, M. Klobukowski, and S. Huzinaga, J. Chem. Phys. **106**, 8084 (1997); E. Miyoshi, Y. Sakai, K. Tanaka, and M. Masamura, J. Mol. Struct.: THEOCHEM **451**, 73 (1998); Y. Sakai, E. Miyoshi, and H. Tatewaki, *ibid.* **451**, 143 (1998).
[17] S. Huzinaga, Can. J. Chem. **73**, 619 (1995); M. Klobukowski, S. Huzinaga, and Y. Sakai, in *Computational Chemistry: Reviews of Current Trends*, edited by J. Leszczynski (World Scientific, Singapore, 1999), Vol. 3, pp. 49–74; C. C. Lovallo and M. Klobukowski, J. Comput. Chem. **24**, 1009 (2003); **25**, 1206 (2004).
[18] S. A. Decker and M. Klobukowski, J. Chem. Inf. Comput. Sci. **41**, 1 (2001).
[19] Y. Osanai, T. Noro, and E. Miyoshi, J. Chem. Phys. **117**, 9623 (2002).
[20] D. G. Fedorov and M. Klobukowski, Chem. Phys. Lett. **360**, 223 (2002).
[21] S. Koseki, Y. Ishihara, H. Umeda, D. G. Fedorov, and M. S. Gordon, J. Phys. Chem. A **106**, 785 (2002); S. Koseki, Y. Ishihara, H. Umeda, D. G. Fedorov, M. W. Schmidt, and M. S. Gordon, *ibid.* **108**, 4707 (2004); S. Koseki, T. Matsushita, and M. S. Gordon, *ibid.* **110**, 2560 (2006); S. Koseki and M. S. Gordon (unpublished).
[22] S. Koseki, M. W. Schmidt, and M. S. Gordon, J. Phys. Chem. **96**, 10768 (1992); S. Koseki, M. S. Gordon, M. W. Schmidt, and N. Matsunaga, *ibid.* **99**, 12764 (1995); N. Matsunaga, S. Koseki, and M. S. Gordon, J. Chem. Phys. **104**, 7988 (1996); S. Koseki, M. W. Schmidt, and M. S. Gordon, J. Phys. Chem. A **102**, 10430 (1998); S. Koseki, D. G. Fedorov, M. W. Schmidt, and M. S. Gordon, *ibid.* **105**, 8262 (2001).
[23] S. Koseki, *Computational Methods in Sciences and Engineering, Theory and Computation: Old Problems and New Challenges*, edited by G. Maroulis and T. Simos, (■, ■, 2008), Vol. 1, p. 257; S. Koseki, N. Shimakura, Y. Fujimura, T. Asada, and H. Kono, J. Chem. Phys. **131**, 044122 (2009).
[24] T. Hisashima, T. Matsushita, T. Asada, and S. Koseki, Theor. Chem. Acc. **120**, 85 (2008).
[25] T. Matsushita, T. Asada, and S. Koseki, J. Phys. Chem. A **110**, 13295 (2006); J. Phys. Chem. C **111**, 6897 (2007).
[26] S. Koseki, T. Asada, and T. Matsushita, J. Comput. Theor. Nanosci. **6**, 1352 (2009); T. Asada, S. Hamamura, T. Matsushita, and S. Koseki, Res. Chem. Intermed. **35**, 851 (2009).
[27] X. Wang and L. Andrews, J. Phys. Chem. **107**, 4081 (2003).
[28] Y. Kuninobu, A. Kawata, and K. Takai, J. Am. Chem. Soc. **127**, 13498 (2005); Y. Kuninobu, Y. Tokunaga, A. Kawata, and K. Takai, *ibid.* **128**, 202 (2006); Y. Kuninobu, Y. Nishina, M. Shouho, and K. Takai, Angew. Chem., Int. Ed. ■, ■ (2006); Y. Kuninobu, A. Kawata, and K. Takai, Org. Lett. **7**, 4823 (2005).
[29] T. Oshiki, H. Yamashita, K. Sawada, M. Utsunomiya, K. Takahashi, and K. Takai, Organometallics **24**, 6287 (2005).
[30] The exponent of 0.869 was used for *f* functions in Re atom.
[31] H. Nakano, J. Chem. Phys. **99**, 7983 (1993).
[32] Unfortunately, first-order or second-order configuration interaction wave functions could not be used, since it is too time-consuming to carry out such calculations in our laboratory.
[33] The SOC matrices include all electronic states that total energies are lower than −80.190 hartree.
[34] M. W. Schmidt, K. K. Baldridge, J. A. Boatz, S. T. Elbert, M. S. Gordon, J. H. Jensen, S. Koseki, N. Matsunaga, K. A. Nguyen, S. Su, T. L. Windus, M. Dupuis, and J. A. Montgomery, J. Comput. Chem. **14**, 1347 (1993).
[35] There is the arbitrariness that irreducible representations of D_{2h} point group depend on the choice of coordinate axes.
[36] H. Köuppel, L. S. Cederbaum, and W. Domcke, Adv. Chem. Phys. **57**, 59 (1984).
[37] D. R. Yarkony, Int. Rev. Phys. Chem. **11**, 195 (1992); J. Am. Chem. Soc. **114**, 5406 (1992); D. R. Yarkony, *Conical Intersections*, edited by W. Domcke, D. R. Yarkony, and H. Köppel (World Scientific, New Jersey, 2004), Chap. 3, p. 129.
[38] N. Matsunaga and D. R. Yarkony, J. Chem. Phys. **107**, 7825 (1997); Mol. Phys. **93**, 79 (1998).

AQ: #12
AQ: #13
AQ: #14
AQ: #15

AUTHOR QUERIES — 056037JCP

#1 Au: Please check changes in full title, byline and affiliations.
#2 Au: Abstract must be self-contained. Please check our insertion.
#3 Au: Please check definition of DFT added.
#4 Au: Please cite specific section if possible.
#5 Au: Please check display equation that follows.
#6 Au: Please cite specific sections if possible.
#7 Au: Please verify citation of Sec. IIIA.
#8 Au: Please cite specific section if possible.
#9 Au: Please cite specific section if possible.
#10 Au: Please cite specific sections if possible.
#11 Au: Please verify that the first author should be ″Heß″ not ″Hess″ in Ref. ″Hess, Marian, Peyerimhoff, 1995″.
#12 Au: Please update Ref. 21(d) if possible.
#13 Au: Please provide publisher and location for Ref. 23(a) and check page no. in Ref. 23(b).
#14 Au: Please provide volume and page no. for Ref. 28(c).
#15 Au: Please verify accuracy of author in Ref. 36.
#16 Au: Please check changes in Table I.
#17 Au: Please check changes in Table II.